International Journal of
INTELLIGENT SYSTEMS AND APPLICATIONS IN ENGINEERING
ISSN:2147-6799 www.ijisae.org Original Research Paper

FS (CA)^2 Net: Feedback Spatial Channel Attention and Context Attribute Extraction System for Skin Lesion Segmentation in Melanoma

Bhargav Kandala*[1], Raj Kumar G. V. S.[2]

Submitted: 16/01/2024 **Revised**: 24/02/2024 **Accepted**: 02/03/2024

Abstract: Melanoma is known as the most common type of disease, which is currently prevalent globally. Early detection of these disorders is crucial to saving lives. Visual inspection of such lesions during medical tests is challenging due to the overlap of lesions. Current advanced research has suggested the importance of Deep Learning in various real-time applications. Moreover, it has emerged as one of the promising methods to achieve cutting-edge outcomes in several medical applications. In this work, we focus on the development of an oriented methodology for skin lesion segmentation to improve the overall segmentation accuracy. The traditional DL-based methods have reported a gradual increase in segmentation accuracy, but computational complexity and degradation in accuracy due to skin hair and borders remain challenging tasks. Therefore, we present a novel DL-based scheme that is based on the UNet architecture. The UNet-based architectures have reported noteworthy performance for medical image segmentation tasks, but spatial and contextual information collection and processing remain tedious for this process. To overcome this issue, we incorporate channel and spatial attention modules along with the feedback process, which helps to improve the skip connection process by retaining the feature map information. The proposed FS (CA)^2 Net architecture is evaluated on different datasets, and experimental study shows that the proposed FS (CA)^2 Net achieves 0.96, 0.99, and 0.94 dice scores for PH^2, ISIC 2017, and HAM10000 datasets, respectively.

Keywords: *Skin Lesion Segmentation, Melanoma, UNet, Deep Learning, Computer Vision*

1. Introduction

Tumor malignancy is the second leading cause of deaths in America and a substantial worldwide public health concern [1]. In year of 2019, the world has witnessed the pandemic caused due to coronavirus disease which has triggered the delay in diagnosis and cure of the cancer due to closures of healthcare facilities, employment turmoil, overburdened insurance companies and risk of coronavirus infection. However, the spread of COVID-19 was at peak in mid-2020 but still the healthcare facilities and resources are still struggling to rejuvenate the systems. This lead to increase the delay which may cause the increase in advanced stage illness and mortality. These and other pandemic-related side effects will manifest gradually over time and take several years to quantify at the population level due to the 1-2 year latency in population-based cancer rates and fatality rates. Recently, American Cancer Society reported that around 1,958,320 innovative cancer cases and 609,810 mortalities due to cancer are anticipated to transpire in the United States [1]. Skin cancer is a highly perilous condition that, if not detected early, can result in fatal consequences. This invasive disease is caused by the body's melanocyte cells proliferating abnormally. After that, this aberrant cell proliferation multiplies and spreads, penetrating the lymph nodes and destroying the tissues around them [2]. The consequences of these injured cells show up as a raised mole on the skin's outermost layer that can be classified as benign or cancerous. Notably, the most common types of skin cancer include melanoma (MEL), basal-cell carcinoma (BCC), non-melanoma skin cancer (NMSC), and squamous-cell carcinoma (SCC). The accompanying figure illustrates the widespread occurrence of various types of cancers [3].

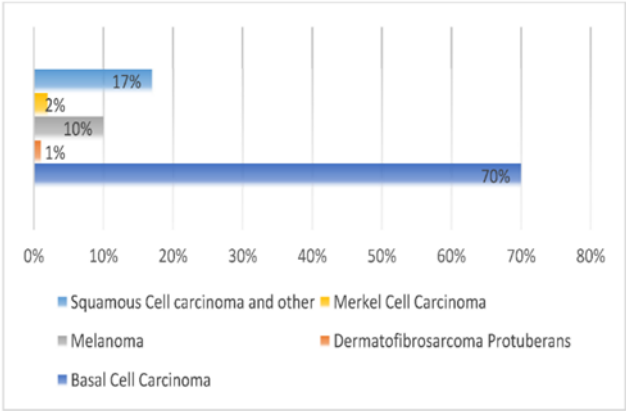

Fig. 1. Different Types of Cancer Widespread

Skin cancer is globally prevalent dangerous disease because according to a study presented in [4] reported that 300,001 more diagnosis cases and 1 million mortalities globally. Melanoma is now the 19th most frequent illness globally and has the uppermost humanity percentage [4]. According to the data from the International Agency for Research on Cancer (IARC) [5], there were expected 19.3 million innovative instances of cancer identified and a 10-million-

[1] *Department of Computer Science and Engineering, GITAM School of Technology, GITAM (Deemed to be University) Visakhapatnam, India*
ORCID ID : 0000-0003-2634-5552
[2] ** Corresponding Author Email: bkandala@gmail.com*

person death rate in the year 2020. Additionally, there were 100,350 innovative belongings identified in the US, and roughly 6850 individuals died in 2020. The ACS (American Cancer Society) reported identification of 106,120 innovative examples of melanoma in 2021 which comprises everywhere 62,260 and 43,850 men and women, and 7180 fatalities in melanoma affected role [6].

Invasive malignant melanoma cases were predicted to total 97,610 in the US in 2023, a small decrease from the predicted 99,780 cases in 2022, but with an increase in fatalities from 7650 in 2022 to 7990 in 2023 [7]. For 2023, 89,070 instances of early in situ melanoma were anticipated. Detected and treated melanoma at this point are completely treatable. Moreover, this study has reported the early in situ melanoma cases as 89,070. The melanoma detection in this stage is important because it is entirely curable in this stage. The projected melanoma incidence count is only anticipated to rise. By 2040, melanoma is predicted to overtake lung cancer as the second most prevalent kind of cancer [8]. Compared to Black Americans, Caucasian people have a more than 20-fold higher melanoma prevalence. For Caucasians, the generation risk of acquiring melanoma is about 2.6 percent, 0.1 percent for Blacks, and 0.6 percent for Hispanics [7].

Similarly, according to the Indian Council of Medical Research's (ICMR) 2021 study, compared to other parts of the globe, melanoma frequency in Indian regions is minimal relative to all other cancers. This research examined data from India's Population-Based Cancer Index. They discovered that the Northeast of India has the greatest incidence 5.14 for men and 3.98 for females. The prevalence of 6.2 was higher among men in the East [9].

1.1. Skin Cancer, its Types and Stages

As discussed before, melanoma is a kind of malignancy of skin that occurs because of abnormal growth of melanocyte cells in the physique. Generally, this irregular growing is divided into three categories as: (a) basal cell carcinoma, (b) squamous cell carcinoma, and (c) melanoma. It is shown in Figure 2 , the example of these cases.

(a) Basal Cell Carcinoma: As older skin cells disappear; a type of cell called a basal cell in the skin is in charge of producing new ones. One type of skin cancer that develops in the basal cells is called basal cell carcinoma. Most basal cell carcinomas are thought to have their primary etiology in prolonged sun exposure. [10].

(b) Squamous Cell Carcinoma: A rather prevalent kind of squamous cell skin cancer. The middle and outer layers of the skin are formed by these cells. Although this particular cancer is not thought to be fatal, if treatment is not received, it may become aggressive and have major side effects.

(c) Melanoma: It is very complex kind of skin cancer which evolves in the melanocytes cells. These cells are answerable to provide the pigmentation to skin. Melanoma can spread in different body parts such as eyes, nose and throat etc. [11].

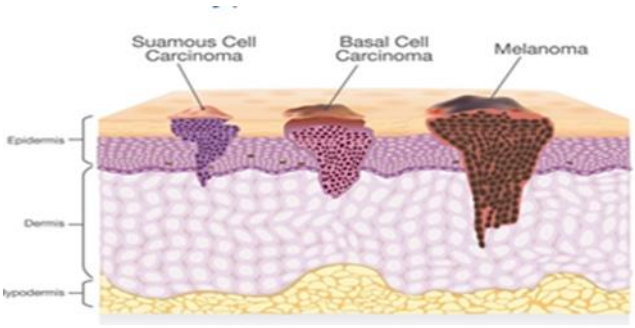

Fig. 2. Types of Skin Cancer

The uncontrollable growth of cancerous cells create difficulty to manage appropriate diagnosis. Fortunately, the abnormal growth appears on the skin surface therefore it is easier to analyze it through simple visual inspections and it can be fully recovered in its initial phases. However, the presence of melanoma is ensured through biopsies of suspected lesion or mole [12]. The melanoma is further categorized into four stages which are obtained based on four basic characteristics such as tumor thickness, spread to lymph nodes, ulceration, spread to other body parts [13]. Below given table 1 presents the brief discussion about these stages and figure 3 depicts the examples of these cases.

Table 1. Various Stages of Melanoma

Stages & Description	
Stage 0	Melanocytes exhibiting abnormalities may be detected within the epidermis, the outer layer of the skin. If these aberrant cells undergo a malignant transformation, this stage is referred to as "melanoma in situ."
Stage I	Melanoma has progressed, with evaluation focusing on ulceration and thickness, distinguishing between Stage IA and Stage IB. Stage IA: The tumor lacks ulceration and is less than 1 mm thick. Stage IB: The tumor either has ulceration but is less than 1 mm thick or exhibits ulceration and is between 1 mm and 2 mm thick.

Stage II	Considering both thickness and ulceration, this stage comprises Stage IIA, Stage IIB, and Stage IIC. Stage IIA: The tumor is either larger than 1 mm but not exceeding 2 mm in thickness or falls between 2 mm and 4 mm in thickness without ulceration. Stage IIB: The tumor is either more than 2 mm thick but not exceeding 4 mm with ulceration, or it surpasses 4 mm in thickness without ulceration. Stage IIC: The tumor exhibits both ulceration and a thickness greater than 4 mm.
Stage III	Inspect the aspect of metastasis. The tumor, regardless of ulceration, may have variable thickness. The primary tumor has the potential to metastasize to any part of the lymphatic system, with melanoma cells spreading 2 cm or more from the main cancer site. Additionally, the connection of minor tumors on or beneath the epidermis, within a 2 cm radius of the initial tumor, is also a conceivable scenario.
Stage IV	Cancerous metastasis may have affected organs such as the liver, lungs, brain, and others, some of which could be distant from the primary tumor site.

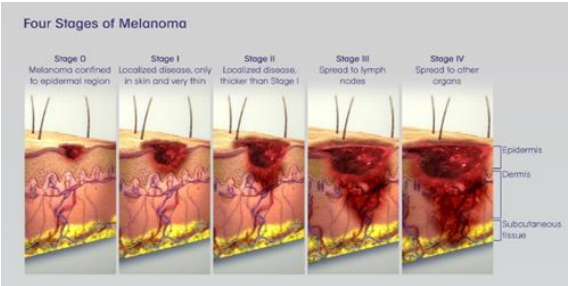

Fig. 3. Different Stages of Melanoma

1.2. CAD, Dermoscopy with Computer Vision-Based AI Scheme for Skin Cancer

Several researchers have reported the importance of early detection of skin abnormality to facilitate the full recovery from skin cancer. Moreover, the prompt discovery aids in raising the rate of survival more than 95.1% [14]. Generally, this inspection is performed on skin lesion images; consequently, precise investigation of these images plays a significant role in early detection. After skin imaging is conducted, dermatoscopy emerges as a hopeful explanation due to its ability to afford exaggerated skin images, characteristically at a factor of x10.

However, the conventional methods require more time, and effort. Moreover, the detection accuracy is subjective to the expert skills. Therefore, automating this process while maintaining desire accuracy is considered as the important task for researchers. In traditional clinical practices, ABCDE measurement parameters are widely adopted which represents the several metrics such as colour, border, diameter over 6mm, asymmetry, and development. Though, it requires high level of expertise and knowledge. Furthermore, Dermatologists' aptitude to precisely notice skin lesions is described fewer than eighty percent of the time [15]. Also, there is a dearth of qualified dermatologists in the medical field worldwide. Several research contributions have been presented in literature according to the computer vision-based approaches to identify the skin lesion abnormalities in its early stages [16].

In instruction to obtain the desired accuracy, skin lesion division actings important part to extract the region of Interest. Traditionally, several methods Techniques have been demonstrated for segmenting skin lesions, including thresholding technique, fuzzy logic, gradient vector flow (GVF) snakes, clustering, region growing and active contour etc. Despite of their prevalence, the outcome of these methods rely on the handcrafted features. Moreover, these methods suffer from issue of poor accuracy. Currently, DL based methods have gained huge attention in numerous computer visualization based responsibilities such as surveillance [17], biomedical image processing, data mining and many more. Therefore, this work mainly focusses on adopting the deep knowledge scheme for skin lesion division.

1.3. Article Organization

Remainder of object is arranged in subsequent sections: section II provides a review of the literature on skin lesion segmentation, section III presents the planned CNN based architecture for skin image pre-processing and melanoma segmentation, section IV presents the experimental analysis where outcome of suggested method is contrasted with the existing DL based skin tumor segmentation schemes and lastly, section V grants the closing comments and upcoming

research direction.

2. Literature Survey

This segment makes a short-term discussion on current schemes of melanoma image segmentation. As discussed in previous section that the traditional segmentation schemes are not suitable to handle the complex structured images and achieving the desired accuracy remained challenging task. Therefore, the advanced studied has suggested the importance of deep learning methods. This segment describes the deep learning founded melanoma division methods.

Generally, the image segmentation task is considered as classification problem but the traditional segmentation methods require dense prediction therefore Ronneberger et al. [18] introduced deep learning based model known as UNet which is widely adopted in biomedical image segmentation. This module contains encoder module where downsampling process is used in capturing the semantics and contextual information, similarly, it contains expanding path that is connected to the downsampling path and used to obtain the accurate localization information of ROI. This convolution design involves the encoder and decoder modules to obtain the semantic segmentation. Currently, several advancements have been incorporated to this architecture to increase the segmentation accuracy. In this context, Zhou et al. [19] modified the UNet architecture and introduced UNet++ where dense skip influences are redesigned to mitigate the semantic divide amid charateristics representation and encoder-decoder networks.

The skip connection plays important role while focusing of the feature information. Therefore, Wei et al. [20] adopted an attention mechanism which is used in skip connection to increase the focus on identifying the best region for segmentation. This is helpful in detecting even smaller objects. Based on this concept authors introduced attention module integrated DenseUNet architecture along with adversarial training. This architecture follows the concept of Generative Adversarial Network as it contains segmentor and discriminator modules. The segmentor block uses DenseNet design to extract the multiscale information and attention layer helps concentrating only on the skin lesion characteristics and discards other features. Similarly, the discriminator block uses adversarial feature matcher to improve the stability of segmentation module. Further, it uses a unique loss function by combining the jaccard distance loss with the adversarial characteristics.

Alahmadi et al. [21] reported that the traditional UNet based methods have poor performance for multi-scale objects with large variation in shape and texture. Therefore, authors developed multiscale UNet. This model also adopted attention mechanism which is used in aggregating the multi-level picture to adjust the important topographies. Further, this model uses Bidirectional Convolutional Long Short-term Memory (BDC-LSTM) to extract the judicial characteristics.

Ren et al. [22] presented channel and spatial attention mechanism and introduced a novel approach to connect the attention modules serially. Further, the combined attention modules are embedded into skip connection of encoder-decoder network.

Chen et al. [23] constructed Recurrent Attentional Convolutional Networks to exploit the attention class features with the help of O-shape structure. Further, attention class feature module is also proposed which is integrated in the network architecture. The O-Net refines the segmentation outcome iteratively based on the attention feature information.

Wu et al. [24] introduced a Feature Adaptive Transformer Network (FAT-Net) design in their work that is established on the traditional encoder-decoder modules to efficiently capture global context information and long-term relationships by incorporating an additional transformer outlet. This method practices feature fusion component and reminiscence effective decoder to fuse the adjacent level characteristics. Thus, they turn on the necessary channels and supress the surrounding noise.

Ramadan et al. [25] reported that UNet fail to find the skin border precisely. Therefore, the authors presented a new model of Unet called Dual Gradient-Color U-Net (DGCU–Net) that involves two encoder modules and a single decoder path. This model relies on the color and gradient info of the test image for identification of the skin border. The obtained gradient information is used to compute the attention maps to strengthen the colour attributes. The encoder and decoder modules are coupled through Atrous spatial pyramid pooling, and connections are strengthened by incorporating spatial and channel attention models.

Gu et al. [26] introduced an complete deep edge CNN architecture for skin lesion segmentation. This architecture uses encoder-decoder modules along with the attention mechanism to detect the lesion boundaries. The decoder phase contains an Edge Information Guided Module (EIGM) to consider the border info of the innovative image. Further, this information is fused with diverse layers of contextual info. Finally, Entirety-Center-Edge (ECE) loss purpose is defined for retaining the boundary information and optimizing it to obtain the final segmentation output.

3. Proposed Model

Preceding unit has described the prevalence of skin cancer and present progressions to improve the various issues faced during diagnosis process. The technological advancements have suggested to incorporate to adopt machine learning based methods to solve different types of medical image

processing tasks. However, the traditional machine learning schemes fail to achieve the desired performance due to several issues. Therefore, researchers have developed deep learning based approaches where the segmentation task is divided into pixel classification task. These deep learning based methods have overcome the issues of existing machine learning methods. However, these methods suffer from accuracy related issues in skin melanoma segmentation due to boundary, hair, poor contrast, ambiguity in skin lesions etc. Therefore, we focus on improving the segmentation accuracy by adopting the deep learning method. This section presents the proposed perfect for skin lesion segmentation.

3.1. Overview of UNet Architecture

UNet is based on the process of neural network which consist of symmetric encoder and decoder modules. This model has improved the medical image analysis significantly. It contains contacted paths to extract the features. Similarly, the extended paths help to enable the localization. The central portion of this network uses skip-connection that is used to attach the encoder and decoder branches. Moreover, it helps to pass the high resolution information in the entire network. Skip connection helps to fetch the spatial attributes which are lost amid the pooling processes, resulting in improving the learning process. Below given figure 4 depicts the standard UNet architecture.

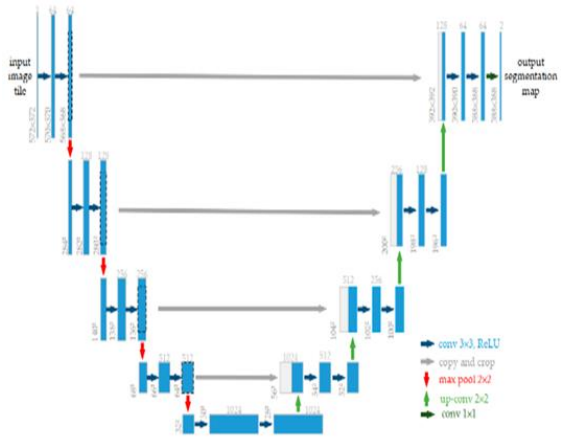

Fig .4. Standard UNet Architecture

3.2. Attention Mechanism

Attention mechanism is considered as one of the promising method in human perception. This method helps humans to focus on the certain key information and ignore irrelevant information. This helps to accelerate the learning process of deep CNN, extract the critical information, and enhance the robustness of learning network. below given figure shows the three different attention modules.

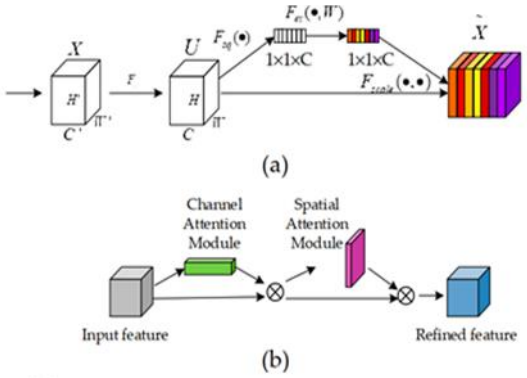

Fig. 5. Attention mechanism (a) Convolution Attention Module (b) Spatial Attention(SA) & Channel Attention (CA)

According to the process mentioned in figure 5(a) channel convolution attention process focus on estimating the channel relationships between image features and figure 5 (b) presents a combined channel and spatial attention module. Generally, the traditional attention mechanisms start from the single focus but as the skin lesion images have several complications such as uneven colour distribution, blurred boundaries, irregular shapes therefore the single focus attention schemes do not perform well. Therefore, we present an integrated attention mechanism.

3.3. Proposed FS (CA)^2 Net for Lesion Segmentation

The suggested deep learning architecture for segmenting skin tumors is shown in this section. The suggested architecture is based on the UNet model, into which we have included a contextual attribute extraction model, a feedback-aware skip connection, and an attention mechanism. The suggested deep learning model's design is shown in figure 6 below.

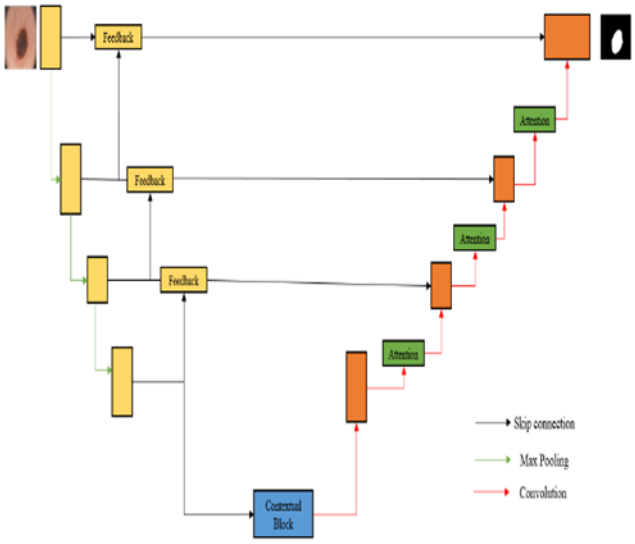

Fig. 6. Proposed FS (CA)^2 Net Architecture for Segmentation

The proposed model uses feedback module during down sampling phase which helps to obtain the rich feature

information. Similarly, the attention block is practical in the up-sampling process to find the vital info of the feature map (FM). The main contribution of proposed work lies in feedback model during down sampling and integrated attention module during upsampling to analyse the feature maps efficiently.

(a) Feedback Module

As discussed before, the UNet is based on encoder and decoder based setup which is adopted to obtain the attributes and characteristics of the input data. The entire network can be examined into two primary components, a decoder and an encoder. In encoder, it performs the down sampling process where two main operations convolution and pooling are performed. However, during this process, some critical information is missed or ignored. Moreover, the complexity in skin lesions also affects the process of global feature extraction. To overcome these issue, we present a feedback module which is based on the concept of reusing the feature information. The Feature Pyramid Network (FPN) model also follows this process by employing the top-down procedure. The obtained feature maps are up-sampled and added together from the feed-forward feature map. Whereas, in proposed module follows a top-down feedback module where the feature map of upper module is connected back to the lower level. This process helps to obtain the rich feature information. Further, these attributes are combined with the feedback module and merged with the resultant upsampling layer with the help of skip connection. Below given Fig. 7 shows the architecture of feedback module.

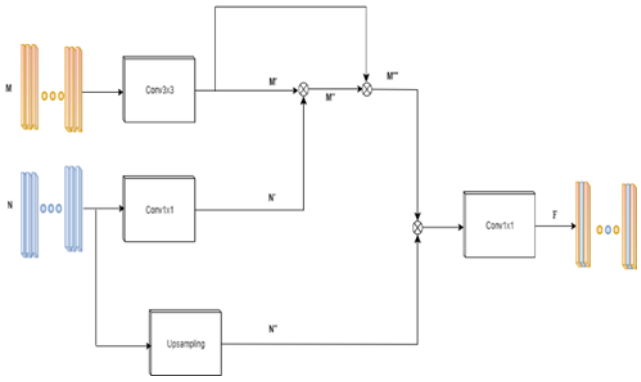

Fig. 7. Feedback Module for Reusing the Feature Information

This module contains two parts as input from encoding layer E1, and E2. The output of encoding layer E1 represents the feature map as $M \in R^{C\times H\times W}$ w which is considered as the input to the first part. This feature map is processed through the various convolution operations. This process produces the features M' without varying the channel and resolution configuration. The obtained resolution is spliced with feature weight map $N' \in R^{C\times 1\times 1}$. This product helps to produce the improved FM as $M'' \in R^{C\times H\times W}$. further, this FM is integrated with the actual FM to attain the final aggregated FM as $M''' \in R^{2C\times H\times W}$ as output from first part.

Similarly, in second path the given feature map is $N \in R^{2C\times\frac{H}{2}\times\frac{W}{2}}$ is used as input. This FM focus on extracting the supreme worth of respectively channel with the help of global pooling and 1x1 convolution operations. In addition, we process the actual feature map through the up-sampling layer which generates a resultant new FM as $N'' \in R^{2C\times H\times W}$. Lastly, the feature map M^'" and N^" are combined composed and the FM is generated as $F \in R^{C\times H\times W}$ input, output and their corresponding operations are presented in below given table 1.

Network Parts	Operations	Input	Output
Part 1	Conv3X3, Element wise multiplication and concatenation	C X H X W C X H X W & C X 1 X 1 C X H X W & C X H X W	C X H X W C X H X W 2C X H X W
Part 2	Gap Con1X1	2C X H/2 X W/2 2C X 1 X 1 2C X H/2 X W/2	2C X H X W C X H X W 2C X H X W
Connection	Concat Conv1X1	2C X H X W & 2C X H X W 4C X H X W	4C X H X W C X H X W

Table. 1. Various Operations of Feedback Module

(b) Attention Mechanism

In this work, we incorporate attention mechanism due to its several advantages in computer vision based applications. below given figure 8 shows the architectural representation of attention module which is obtained by combining channel and spatial attention modules.

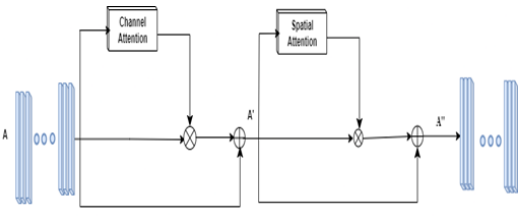

Fig. 8 Attention Mechanism

The output of upsampling feature map is given as input to this block as $A \in R^{C\times H\times W}$. In first phase, we compute the

weight and feature maps with the help of channel attention module. The obtained weight is expressed as $W_C \in R^{C\times1\times1}$ and FM $A' \in R^{C\times H\times W}$. Later, A^' is given as input to the SA block which generates the weighted image of spatial attributes as $W_p \in R^{C\times1\times1}$. Finally, the product of W_p and A^' produces the last output map as $A'' \in R^{C\times H\times W}$. Figure 9 depicts the architecture of CA and SA modules.

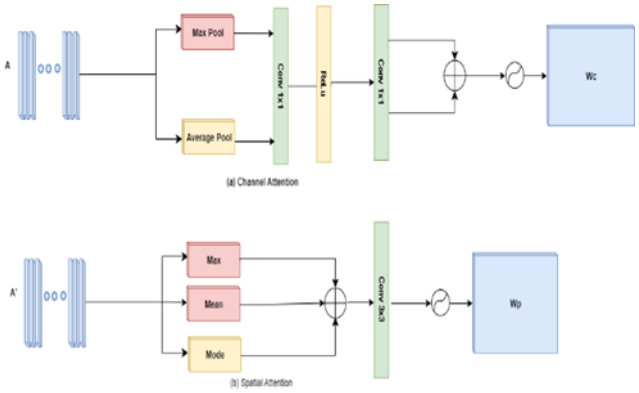

Fig. 9. Channel and Spatial Attention Modules

4. Results and Discussion

This section assesses performance of the future deep learning architecture and validates it by applying the proposed mechanism on publically available dataset.

4.1. Dataset Details

In this effort, we have used 3 distinct datasets for performance evaluation which includes PH2 dataset, ISIC 2017 Dataset and HAM10000 dataset.

PH² Dataset: It contains overall 200 images in which 80 images belongs atypical nevi, 80 images belong to common nevi, and 40 images belong to melanomas. According to the Fitzpatrick skin type classification, all dermoscopic images are either below to skin type II or III. Therefore, the skin colour may vary.

ISIC 2017 Dataset: This dataset contains of 2000 training images and 600 test samples. Ground truth and patient data is included for training and testing. This group consists different categories such as melanoma, nevus or seborrheic keratosis, melanoma or nevus.

HAM10000 Dataset: This dataset consist of 10000 training images which are used to detect the pigmented skin lesions.

4.2. Evaluation Metrics

Five distinct criteria that are frequently used to assess segmentation performance are used to gauge the effectiveness of the proposed model. Here is a description of these metrics:

Dice Similarity Coefficient (DSC): The spatial overall difference between the expected and groundtruth images is computed using this matrix. It is calculated in this way:

$$DSC(S,G) = \frac{2\times|S\cap G|}{|S|+|G|}$$

Intersection Over Union(IoU): The segmentation accuracy is assessed using this matrix, which is also referred to as the Jaccard Index. The ratio of the item to the matching union, which is projected in the same plane, is used to measure it. It is calculated as follows:

$$IoU(S,G) = \frac{|S\cap G|}{|S\cup G|}$$

where G is the ground truth and S is the anticipated mask.

F-Measure: It represents the precision and recall adjusted harmonic mean. It is obtained as:

$$FMeasure = \frac{2\times P\times R}{P+R}$$

Where P is the precision and R denotes the Recall.

Sensitivity: It calculates the proportion of pixels that are correctly classified. It is stated as:

$$Sen(S,G) = \frac{|S\cap G|}{|G|}$$

Specificity (Spe): It calculates the accurate percentage of background class pixels classified correctly. It is said as follows:

$$Spe(S,G) = \frac{|(1-S)\cap(1-G)|}{|1-G|}$$

4.3. Comparative Analysis

The skin hair and the damaged area are captured in the skin lesion photos. The performance of diagnosis is impacted by these kinds of visuals. For hair removal, we thus use an image pre-processing approach. Figure 10 below provides an example of the results of the hair removal method.

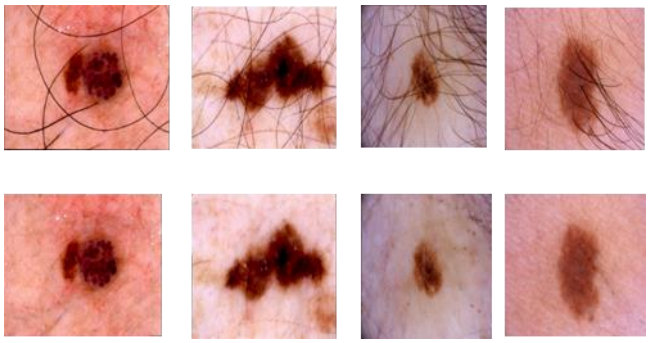

Fig 10. Outcome of Hair Removal Process

For the three distinct datasets under consideration, the suggested approach's performance is contrasted with a number of schemes in terms of DSC, IoU, sensitivity, and specificity. The table below presents a comparative comparison using cutting-edge algorithms.

Data-Set	Methods	DSC	IoU	Sen	Spe

PH²	Double Unet [28]	0.907	0.899	0.945	0.966
	Unet [18]	0.876	0.780	0.816	0.978
	SegNet [29]	0.894	0.808	0.865	0.966
	Ensemble Deep Learning [30]	0.907	0.839	0.932	0.929
	DSNet[31]	-	0.870	0.929	0.969
	DFCNN [32]	0.918	0.848	0.937	0.957
	FCN [33]	0.930	0.871	0.969	0.953
	CNN with Attention Mech. [34]	0.919	0.857	0.963	0.942
	YOLO GrabCut [35]	0.881	0.795	0.836	0.940
	MFSNet [27]	0.954	0.914	0.995	0.997
	FS (CA)²	0.9750	0.9420	0.997	0.998
ISIC 2017	Double Unet [28]	0.913	0.918	0.963	0.974
	Unet [18]	0.778	0.683	0.812	0.805
	SegNet [29]	0.821	0.696	0.801	0.954
	Ensemble Deep Learning [30]	0.853	0.770	-	-
	DSNet[31]	0.938	0.846	-	-
	DFCNN [32]	0.855	0.772	0.824	0.981
	FCN [33]	0.793	0.871	0.899	0.950
	CNN with Attention Mech. [34]	-	0.775	0.875	0.955
	YOLO GrabCut [35]	0.871	0.771	0.854	0.967
	MFSNet [27]	0.987	0.0.974	0.99	0.999
	FS (CA)²	0.9915	0.9840	0.991	0.999
HAM10000	Double Unet [28]	0.843	0.812	0.961	0.845
	Unet [18]	0.781	0.774	0.799	0.802
	SegNet [29]	0.816	0.821	0.867	0.854
	Saha et.al [38]	0.891	0.819	0.824	0.981
	Abraham et.al. [39]	0.856	-	-	-
	Shahin et.al [40]	0903	0.837	0.902	0.974
	Bissoto et.al [41]	0.873	0.792	0.934	0.936
	Ibtehaz et.al. [42]	-	0.803	-	-
	MFSNet [27]	0.906	0.902	0.999	0.99
	FS (CA)²	0.9455	0.9510	0.999	0.998

Table.2. Comparative Performance for Skin Lesion Segmentation

Illustration of utcomes for PH² Dataset

Groundtruth SegNet UNet DoubleUNet MFSNet FS(CA)²

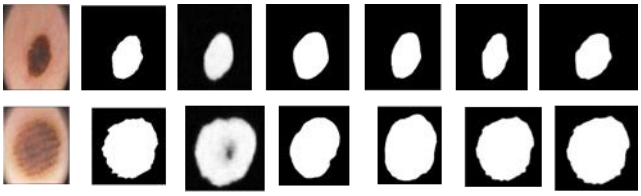

Illustration of Consequences for ISIC 2017 Dataset

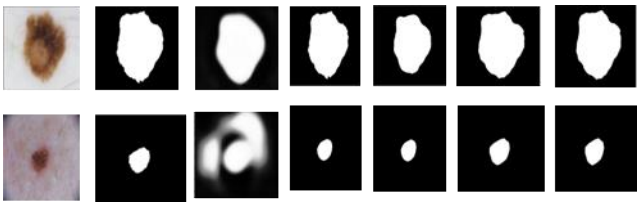

Illustration of Results for HAM 10000 Dataset

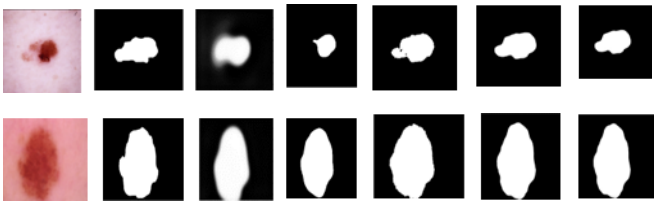

Fig. 11. Sample Outcome for PH², ISIC 2017 and HAM 10000 Dataset

Dataset	Fold	DSC		IoU		FM		Sen		Spe	
		MFSNet	Proposed	MFSNet	Proposed	MFSNet	Proposed	MFSNet	Proposed	MFSNet	Proposed
PH2	1	0.955	0.965	0.917	0.934	0.947	0.950	1.00	1.00	1.00	1.00
	2	0.956	0.960	0.918	0.940	0.941	0.960	0.991	0.995	0.986	0.995
	3	0.951	0.980	0.915	0.951	0.945	0.955	0.995	0.996	0.999	1.00
	4	0.949	0.958	0.920	0.946	0.943	0.951	1.00	1.00	1.00	1.00
	5	0.958	0.965	0.899	0.921	0.941	0.950	0.989	0.991	0.999	1.00
	Avg	0.954	0.9656	0.914	0.9384	0.944	0.9532	0.995	0.9964	0.997	0.999
ISIC 2017	1	0.991	0.995	0.976	0.980	0.989	0.991	1.00	1.00	1.00	1.00
	2	0.985	0.989	0.971	0.985	0.980	0.985	1.00	1.00	0.986	1.00
	3	0.983	0.991	0.967	0.978	0.980	0.991	0.998	0.999	0.999	1.00
	4	0.986	0.991	0.980	0.991	0.991	0.995	0.999	0.999	0.999	0.999
	5	0.990	0.998	0.975	0.981	0.989	0.999	0.987	0.998	0.998	0.999
	Avg	0.987	0.9928	0.974	0.983	0.986	0.9922	0.999	0.992	0.999	0.999
HAM10000	1	0.911	0.935	0.910	0.930	0.905	0.925	1.00	0.999	0.999	0.999
	2	0.900	0.941	0.901	0.955	0.899	0.934	0.997	0.998	0.998	1.00
	3	0.905	0.935	0.903	0.950	0.906	0.945	0.999	0.999	1.00	0.999
	4	0.904	0.940	0.894	0.945	0.892	0.935	1.00	1	1.00	0.999
	5	0.910	0.953	0.900	0.936	0.914	0.941	0.998	0.999	0.998	1.00
	Avg	0.906	0.9408	0.902	0.9432	0.903	0.936	0.999	0.999	0.999	0.994

Table. 3. Comparative Performance for 5-fold Validation

The experimental study presented in table 1 shows that the proposed FS $(CA)^2$ Net approach achieves better performance for the considered PH^2, ISIC 2017 dataset and HAM 10000 dataset. Figure 11 shows the obtained qualitative performance as segmented output image. Similarly, we measure the performance as training loss, training accuracy, validation loss, and validation accuracy. The outcome of this analysis is presented in below given figure 12.

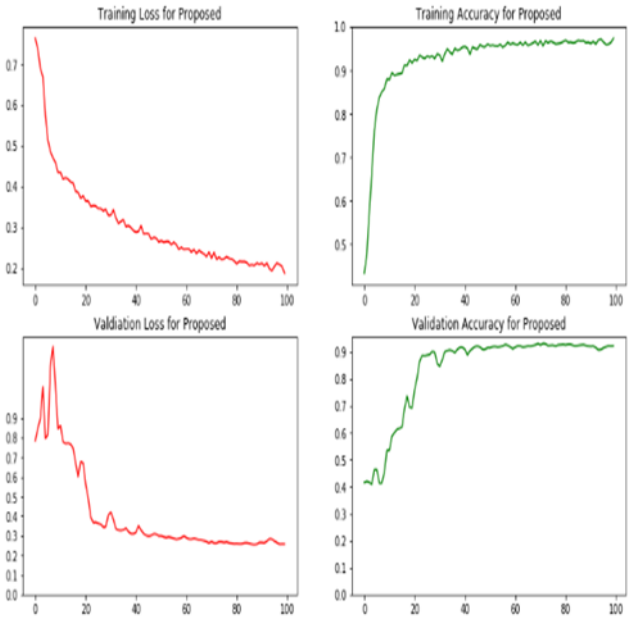

Fig. 12. Training Loss, Training Accuracy, Validation Loss and Validation Accuracy

Further, we extend the performance analysis and evaluated

the outcome of proposed FS $(CA)^2$ Net model for 5-fold cross-validation scenario. The achieved outcome is compared with the existing approach as mentioned in [27]. Below given table 3

demonstrations the proportional investigation for different datasets.

The experimental study has reported that the proposed FS $(CA)^2$ Net system has achieved better accuracy and outperforms the existing DL based approaches for skin lesion segmentation.

5. Conclusion

In this paper, we have implemented a unique computer vision technique based on deep learning to improve the accuracy of melanoma skin cancer detection and segmentation. Given that numerous studies have demonstrated the significance of early cancer identification in lowering the disease's impact and death rate. Therefore, computers vision-based systems are widely adopted to achieve this task. Currently, deep learning has gained huge attention in this field of biomedical image analysis. In this work we adopt the Unet as the base architecture which follows the encoder and decoder process to obtain the final segmentation. However, the traditional UNet fail to achieve the desired performance due to several complexities of skin lesions. To overcome this subject, we familiarize a novel UNet architecture also is known as FS (CA)2. The anticipated architecture uses channel and spatial courtesy module along with the feedback mechanism to improvise the quality of feature map. The investigational study demonstrations that the planned FS (CA)2 method outperforms the traditional deep learning-based segmentation approaches.

References

[1] Siegel, R. L., Miller, K. D., Wagle, N. S., & Jemal, A. (2023). Cancer statistics, 2023. CA: a cancer journal for clinicians, 73(1), 17-48.

[2] Dong, Yuying, Liejun Wang, Shuli Cheng, and Yongming Li. "Fac-net: Feedback attention network based on context encoder network for skin lesion segmentation." Sensors 21, no. 15 (2021): 5172.

[3] Leiter, U., Keim, U., & Garbe, C. (2020). Epidemiology of skin cancer: update 2019. Sunlight, Vitamin D and Skin Cancer, 123-139.

[4] Nikitkina, A. I., Bikmulina, P. Y., Gafarova, E. R., Kosheleva, N. V., Efremov, Y. M., Bezrukov, E. A., ... & Timashev, P. S. (2021). Terahertz radiation and the skin: a review. Journal of Biomedical Optics, 26(4), 043005-043005.

[5] World Cancer Research Fund. (2018). Skin cancer statistics.

[6] International Agency for Research on Cancer. Cancer—World Health Organization. 2020

[7] American Cancer Society. Key Statistics for Melanoma Skin Cancer. 2021.

[8] Siegel, R. L., Miller, K. D., Wagle, N. S., & Jemal, A. (2023). Cancer statistics, 2023. CA: a cancer journal for clinicians, 73(1), 17-48.

[9] Rahib, L., Wehner, M. R., Matrisian, L. M., & Nead, K. T. (2021). Estimated projection of US cancer incidence and death to 2040. JAMA Network Open, 4(4), e214708-e214708.

[10] https://theprint.in/health/india-sees-high-number-of-skin-cancer-cases-in-north-northeast-regions-icmr-study-finds/741687/

[11] Chase, T., Cham, K. E., & Cham, B. E. (2020). Curaderm, the Long-Awaited Breakthrough for Basal Cell Carcinoma. International Journal of Clinical Medicine, 11(10), 579.

[12] Zaidi, M. R., Fisher, D. E., & Rizos, H. (2020). Biology of melanocytes and primary melanoma. Cutaneous Melanoma, 3-40.

[13] Roberts, D. L. L., Anstey, A. V., Barlow, R. J., Cox, N. H., British Association of Dermatologists, Bishop, J. N., ... & Kirkham, N. (2002). UK guidelines for the management of cutaneous melanoma. British Journal of dermatology, 146(1), 7-17.

[14] Treatment, M. (2018). Health Professional Version.(nd) PDQ Adult Treatment Editorial Board. PDQ Cancer Information Summaries [Internet]. Bethesda (MD): National Cancer Institute (US).

[15] Miller, K. D., Siegel, R. L., Lin, C. C., Mariotto, A. B., Kramer, J. L., Rowland, J. H., ... & Jemal, A. (2016). Cancer treatment and survivorship statistics, 2016. CA: a cancer journal for clinicians, 66(4), 271-289.

[16] Kaur, R., GholamHosseini, H., Sinha, R., & Lindén, M. (2022). Melanoma classification using a novel deep convolutional neural network with dermoscopic images. Sensors, 22(3), 1134.

[17] Thomsen, K.; Iversen, L.; Titlestad, T.L.; Winther, O. Systematic review of machine learning for diagnosis and prognosis in dermatology. J. Dermatol. Treat. 2020, 31, 496–510.

[18] Sharma, V., Mir, R. N., & Singh, C. (2023). Scale-aware CNN for crowd density estimation and crowd behavior analysis. Computers and Electrical Engineering, 106, 108569.

[19] Ronneberger, O., Fischer, P., & Brox, T. (2015). U-net: Convolutional networks for biomedical image segmentation. In International Conference 30 on Medical image computing and computer-assisted intervention (pp. 234– 241). Springer

[20] Zhou, Z., Siddiquee, M. M. R., Tajbakhsh, N., & Liang, J. (2018). Unet++: A nested u-net architecture for medical image segmentation. In Deep learning in

medical image analysis and multimodal learning for clinical decision support (pp. 3–11). Springer.

[21] Wei, Z., Song, H., Chen, L., Li, Q., & Han, G. (2019). Attention-based DenseUnet network with adversarial training for skin lesion segmentation. IEEE Access, 7, 136616-136629.

[22] Alahmadi, M. D. (2022). Multiscale attention U-Net for skin lesion segmentation. IEEE Access, 10, 59145-59154.

[23] Ren, Y., Yu, L., Tian, S., Cheng, J., Guo, Z., & Zhang, Y. (2022). Serial attention network for skin lesion segmentation. Journal of Ambient Intelligence and Humanized Computing, 1-12.

[24] Chen, P., Huang, S., & Yue, Q. (2022). Skin lesion segmentation using recurrent attentional convolutional networks. IEEE Access, 10, 94007-94018.

[25] H. Wu, S. Chen, G. Chen, W. Wang, B. Lei, and Z. Wen, ''FAT-Net: Feature adaptive transformers for automated skin lesion segmentation,'' Med. Image Anal., vol. 76, Feb. 2022, Art. no. 102327.

[26] Ramadan, R., & Aly, S. (2022). DGCU–Net: A new dual gradient-color deep convolutional neural network for efficient skin lesion segmentation. Biomedical Signal Processing and Control, 77, 103829.

[27] Gu, R., Wang, L., & Zhang, L. (2022). DE-net: a deep edge network with boundary information for automatic skin lesion segmentation. Neurocomputing, 468, 71-84.

[28] Basak, H., Kundu, R., & Sarkar, R. (2022). MFSNet: A multi focus segmentation network for skin lesion segmentation. Pattern Recognition, 128, 108673.

[29] Jha, D., Riegler, M. A., Johansen, D., Halvorsen, P., & Johansen, H. D. (2020). Doubleu-net: A deep convolutional neural network for medical image segmentation. In 2020 IEEE 33rd International Symposium on Computer-Based Medical Systems (CBMS) (pp. 558–564). IEEE

[30] Badrinarayanan, V., Kendall, A., & Cipolla, R. (2017). Segnet: A deep convolutional encoder-decoder architecture for image segmentation. IEEE transactions on pattern analysis and machine intelligence, 39, 2481–2495

[31] Goyal, M., Oakley, A., Bansal, P., Dancey, D., & Yap, M. H. (2019). Skin lesion segmentation in dermoscopic images with ensemble deep learning methods. IEEE Access, 8, 4171–4181

[32] Hasan, M. K., Dahal, L., Samarakoon, P. N., Tushar, F. I., & Martí, R. (2020). Dsnet: Automatic dermoscopic skin lesion segmentation. Computers in Biology and Medicine, 120, 103738.

[33] Al-Masni, M. A., Al-Antari, M. A., Choi, M.-T., Han, S.-M., & Kim, T.- S. (2018). Skin lesion segmentation in dermoscopy images via deep full resolution convolutional networks. Computer methods and programs in biomedicine, 162 , 221–231.

[34] Öztürk, Ş., & Özkaya, U. (2020). Skin lesion segmentation with improved convolutional neural network. Journal of digital imaging, 33, 958–970

[35] Xie, F., Yang, J., Liu, J., Jiang, Z., Zheng, Y., & Wang, Y. (2020). Skin lesion segmentation using high-resolution convolutional neural network. Computer methods and programs in biomedicine, 186, 105241

[36] Ünver, H. M., & Ayan, E. (2019). Skin lesion segmentation in dermoscopic images with combination of yolo and grabcut algorithm. Diagnostics, 9 , 72.

[37] Bi, L., Kim, J., Ahn, E., Kumar, A., Fulham, M., & Feng, D. (2017). Dermoscopic image segmentation via multistage fully convolutional networks. IEEE Transactions on Biomedical Engineering, 64, 2065–2074

[38] Bi, L., Kim, J., Ahn, E., Kumar, A., Feng, D., & Fulham, M. (2019). Step-wise integration of deep class-specific learning for dermoscopic image segmentation. Pattern recognition, 85, 78–89.

[39] Saha, A., Prasad, P., & Thabit, A. (2020). Leveraging adaptive color augmentation in convolutional neural networks for deep skin lesion segmentation. In 2020 IEEE 17th International Symposium on Biomedical Imaging (ISBI) (pp. 2014–2017). IEEE

[40] Abraham, N., & Khan, N. M. (2019). A novel focal tversky loss function with improved attention u-net for lesion segmentation. In 2019 IEEE 16th International Symposium on Biomedical Imaging (ISBI 2019) (pp. 683–687). IEEE

[41] Shahin, A. H., Amer, K., & Elattar, M. A. (2019). Deep convolutional encoder-decoders with aggregated multi-resolution skip connections for skin lesion segmentation. In 2019 IEEE 16th International Symposium on Biomedical Imaging (ISBI 2019) (pp. 451–454). IEEE

[42] Bissoto, A., Perez, F., Ribeiro, V., Fornaciali, M., Avila, S., & Valle, E. (2018). Deep-learning ensembles for skin-lesion segmentation, analysis, classification: Recod titans at isic challenge 2018. arXiv preprint arXiv:1808.08480

[43] Ibtehaz, N., & Rahman, M. S. (2020). Multiresunet: Rethinking the unet architecture for multimodal biomedical image segmentation. Neural Networks, 121, 74–87